

Electronic Supplementary Information

Paper-based SERS Active Substrates on Demand

*Pushkaraj Joshi and Venugopal Santhanam**

Department of Chemical Engineering,

Indian Institute of Science,

Bangalore-560012

India

Tel: 91-80-2293 3113

Fax: 91-80-2360 8121

*Email: venu@chemeng.iisc.ernet.in

Table of Contents

S1. Data Processing with COBRA code.....	S-2
S2. Effect of thiosulfate treatment (photographic fixer) on SERS	S-3
S3. SERS activity dependence on silver loading	S-4
S4. Concentration dependant SERS activity	S-5
S5. Estimation of Raman Enhancement Factor (EF).....	S-6

S1. Data Processing with COBRA code

Data processing for subtracting the fluorescence background and smoothing was performed using COBRA¹ code executed on MATLAB platform. The following illustration of background correction of R6G adsorbed on tissue paper.

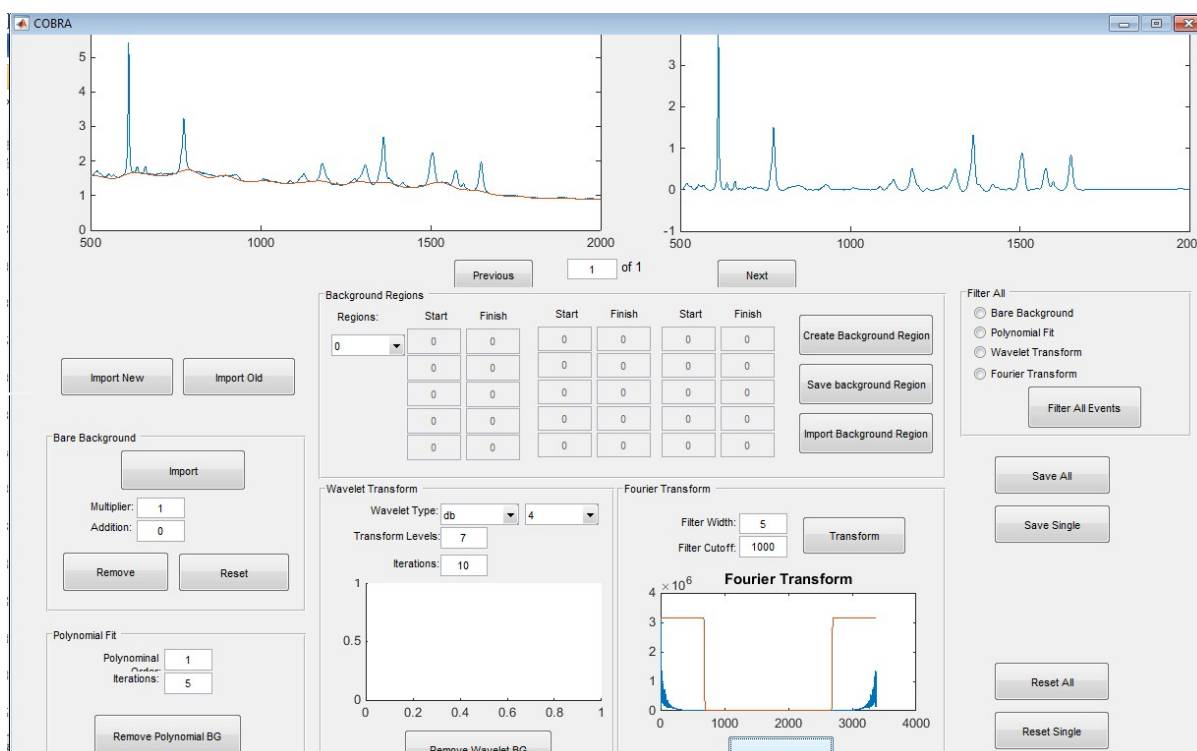


Figure S1. Screenshot showing background correction of a representative spectrum using Wavelet transform and smoothing using Fourier transform.

S2. Effect of thiosulfate treatment (photographic fixer) on SERS

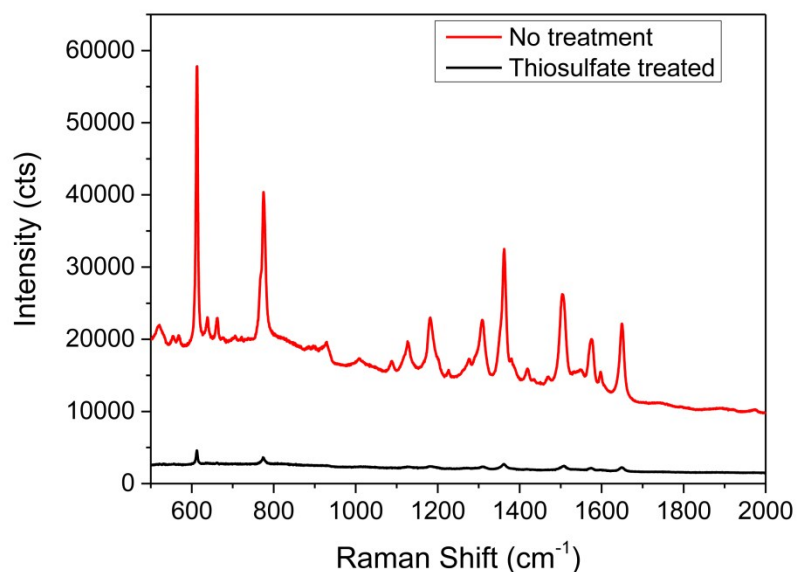


Figure S2a. Effect of treating with thiosulfate solution on developed substrate. SERS spectra taken from substrate soaked in 1 μM R6G solution. Laser power – 250 μW , integration time – 1s.

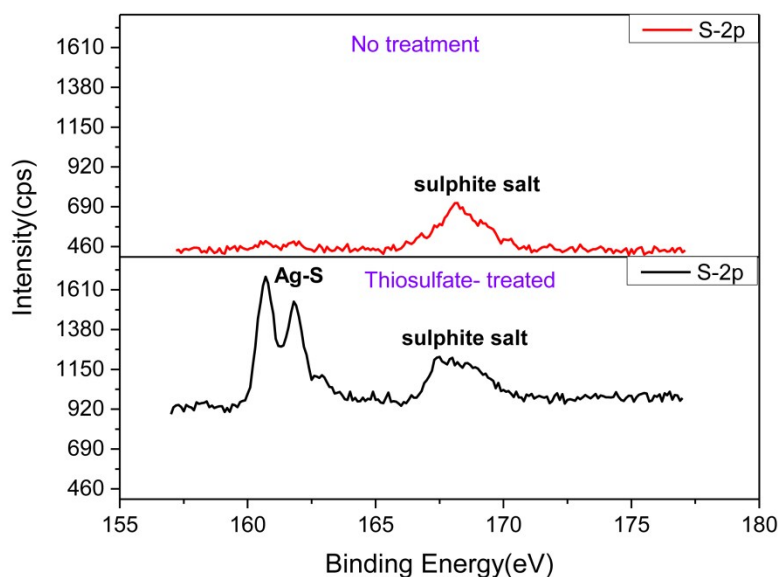


Figure S2b. XPS spectra comparison for untreated and thiosulfate treated substrate. The emergence of metal sulphide species at B.E value of 160.7 eV ($\text{S}2\text{p}_{3/2}$) is attributed to the formation of silver sulphide species after 'fixing'. XPS spectra were collected at a resolution of 0.2 eV, using a Thermo-Scientific Multilab instrument having $\text{AlK}\alpha$ as x-ray source, and charge compensation was carried out using C1s peak at 284.4 eV as the reference value.

S3. SERS activity dependence on silver loading

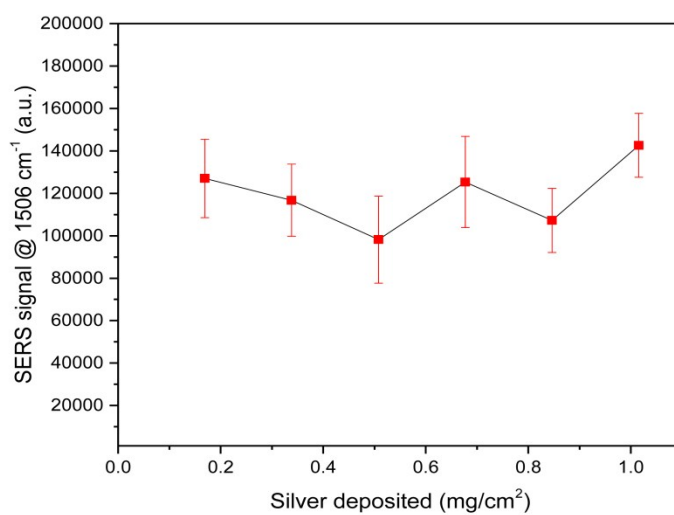


Figure S3. SERS signals obtained from silver nanostructures on Kimwipe[®] tissue paper with different silver loadings. The paper substrates (4mm dia. circle) were dipped in 2 mL of 1 μ M rhodamine 6G solution for 12 hours.

S4. Concentration dependant SERS activity

The model equation used for Langmuir isotherm fit ($R^2 = 99.6\%$) is:

$$I = \frac{I_{max} * C}{(K_d + C)}$$

Where, I is the SERS intensity at concentration C of the R6G solution concentration and I_{max} is the saturating SERS intensity (@1mM R6G), and K_d is the dissociation equilibrium constant. K_{eq} . (the adsorption equilibrium constant) = $1/ K_d$.

Langmuir fit provides $K_d \cong 5.4 \times 10^{-6}$ M; Hence, Adsorption energy $\cong RT \ln(1/K_d) \cong 30$ kJ/mol. This is consistent with the value of 36 kJ/mol reported in literature² for R6G adsorbed onto silver.

Since Langmuir model only allows the formation of monolayer, Total absorbable sites will be filled at saturation. Concentration of adsorbed analytes, at saturation, under laser spot ($1 \mu\text{m}^2$) can be taken as N_{surf} (see S5). So, we can estimate the concentration of adsorbed analyte $C_{adsorbed}$, under laser spot when in contact with solution of analyte concentration C .

Langmuir adsorption model \rightarrow

$$C_{adsorbed} = K_{eq} \times C \times C_{vacant - sites} \quad (1)$$

Site number conservation over a given area \rightarrow

$$C_{Total - adsorbable - sites} = C_{adsorbed} + C_{vacant - sites} \quad (2)$$

Over a $1 \mu\text{m}^2$ area, i.e. laser spot size, \rightarrow

$$C_{Total - adsorbable - sites} = N_{surf} (6.75 \times 10^7, \text{ from S5}) \quad (3)$$

With $K_{eq} \sim 1.8 \times 10^5 \text{ M}^{-1}$; at 100 pM analyte concentration, solving (1), (2) and (3)

$$\rightarrow C_{adsorbed} \sim 1215 \text{ molecules}/\mu\text{m}^2$$

Thus, at 100 pM solution concentration, on average only about 1000 R6G molecules is predicted to be adsorbed onto the surface illuminated by the laser spot!

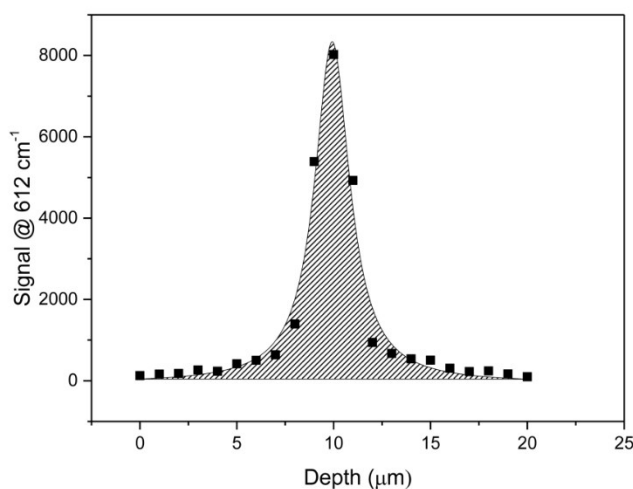
S5. Estimation of Raman Enhancement Factor (EF)

To estimate average EF value of the substrate the following formula is used:

$$EF = (I_{SERS} / I_{bulk}) \cdot (N_{bulk} / N_{surf})$$

Where, I_{SERS} and I_{bulk} are the SERS signals (area under the peak) in the SERS and normal Raman spectra of probe molecule, respectively normalised for acquisition time and laser power density. N_{surf} and N_{bulk} are the number of molecules giving rise to SERS, and the number of molecules in the bulk sample under laser illumination, respectively. The N_{surf} value can be calculated on the basis of the estimated area occupied by probe molecule, and the surface area available for adsorption; while N_{bulk} value has to be estimated from the effective scattering volume in bulk sample and the bulk density of the sample.

Based on the manufacturer's specifications, the laser illuminated spot area $\cong 1 \mu\text{m}^2$. For the solid sample, the sampling volume is the product of the area of the laser spot and the effective height (H_{eff}) probed by the laser beam. H_{eff} is estimated by moving the sample across the laser focus and taking an average of the integrated intensity vs depth profile for the characteristic peak with the maximum intensity as normalising factor³:



$$H_{eff} = \int_{-\infty}^{\infty} I \cdot dz / I_{max}$$

Figure S5a. Raman signal from R6G powder sample obtained by moving laser focus across the sample surface. Laser power – 250 μ W, integration time – 5s.

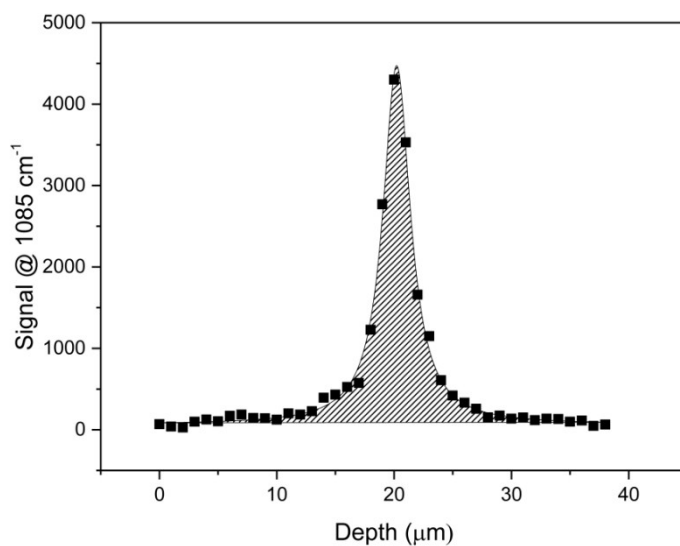
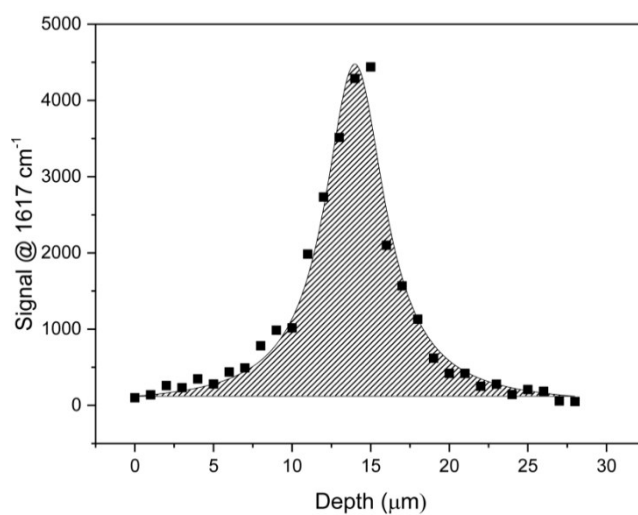


Figure S5b. Raman signal from p-aminothiophenol powder sample obtained by moving laser focus across the sample surface. Laser power – 250 μ W, integration time – 5s.

Figure S5c. Raman signal from malachite green powder sample obtained by moving laser focus across the sample surface. Laser power – 250 μ W, integration time – 5s.



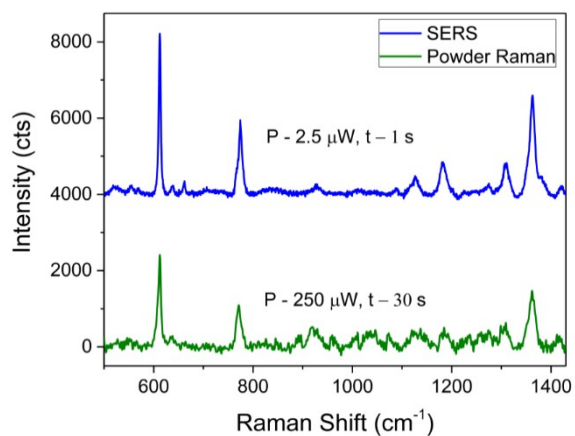


Figure S5d. Comparison of SERS and powder spectra for R6G.

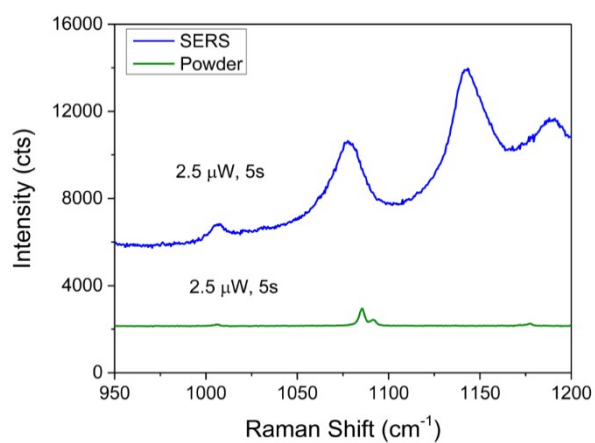


Figure S5e. Comparison of SERS and powder spectra for p-aminothiophenol.

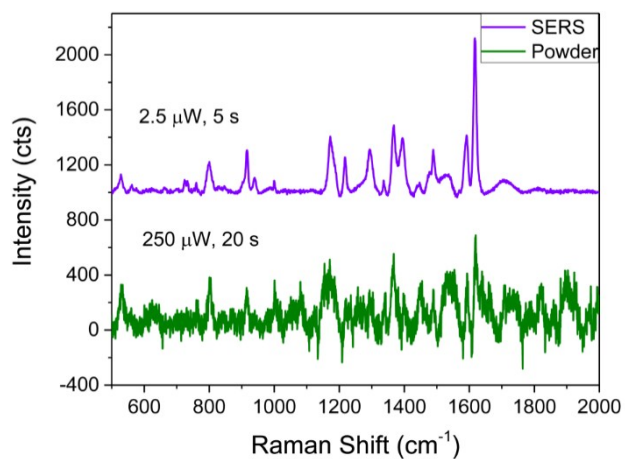


Figure S5f. Comparison of SERS and powder spectra for malachite green.

The characteristic Raman peaks used for computing the EF are 1077 cm^{-1} corresponding to C-S stretching mode for p-ATP,⁴ Normal Raman for p-ATP @ 1085 cm^{-1} corresponds to C-S stretching vibration. The C-S peak is slightly shifted in SERS spectra to 1077 cm^{-1} . This shift can be attributed to adsorption of p-ATP via Ag-S link owing to affinity of Ag towards S-H moiety. Also, SERS spectra shows a peak @ 1142 cm^{-1} which can be attributed to in-plane C-H bending. This peak is very weak in normal Raman and appears only in SERS. For MG,⁵ 1618 cm^{-1} (ring C-C stretching) is used for EF calculation – other characteristic bands like 1397 cm^{-1} (N-phenyl stretching), 1172 cm^{-1} (ring C-H in-plane bending) and 917 cm^{-1} (C-H out-of-plane bending) are also seen. 612 cm^{-1} corresponding to C-C-C ring in plane bending is used for EF calculation for R6G.² Other characteristic R6G bands seen are 774 cm^{-1} (C-H out of plane bending) and 1365 cm^{-1} (ring C-C stretching).

	p-ATP	MG	R6G
N_{bulk}	2.3×10^{10}	1.7×10^{10}	4.9×10^9
Area occupied by molecule ^{6,7}	0.2 nm^2	0.4 nm^2	0.4 nm^2
N_{surf}	5×10^6	2.5×10^6	2.5×10^6
Normalised I_{bulk}	4,120	500	24
I_{SERS}	66,988	10,038	18,472
Enhancement factor	7.5×10^4	1.3×10^5	1.5×10^6

These values are based on geometric footprint area. However, the average EF has to be computed based on an estimate of the actual surface area⁸ available for adsorption. To estimate the roughness factor of silver nanostructures (ratio of actual surface area available for SERS active molecules to adsorb with respect to geometric footprint area), we assumed an average silver wire diameter ($\cong 70\text{ nm}$), based on FESEM measurements, and for the corresponding silver loading of 1 mg/cm^2 , the area available for adsorption is presumed to be the top-half of the length of the silver nanowire of 70 nm diameter required to account for the known silver loading, which is presumed to lie on its side. We calculate the surface area by utilizing the diameter of silver wire and using the density of bulk silver (ρ). We

hereby calculate the total coiled length of silver wire, assuming a model where entire space is filled with a single coiled silver nanowire of 70 nm diameter.

$$1 \frac{mg}{cm^2} = \frac{(\pi r^2 L) * \rho}{1 cm^2} mg$$

$$L = \frac{1}{\rho * \pi r^2} cm$$

Total length of wire on 1 cm² area,

Total surface area available for adsorption of SERS active molecules on silver deposited over

$$\text{geometric area of } 1 \text{ cm}^2 = \pi r L = \pi r * \frac{1}{\rho * \pi r^2} \text{ cm}^2 \cong 27 \text{ cm}^2$$

Hence, Roughness factor = 27.

Roughness corrected enhancement factor for R6G $\cong 5.6 \times 10^4$

Roughness corrected enhancement factor for MG $\cong 4.8 \times 10^3$

Roughness corrected enhancement factor for p-ATP $\cong 2.8 \times 10^3$

To evaluate the advantage of using silver nanowire network, a comparison is made with sputtered silver film 200 nm thick deposited on glass slide by RF sputter coating system (Tecport- Symphony Sputter coater). The film is highly conductive with densely-packed silver nanoparticles exposed in the top layer (Fig. S5g). The Raman signal from 1mM R6G on fabricated SERS substrate and sputter coated silver film on glass is compared in Fig. S5h.

$$\text{Nanostructured Advantage} = \frac{I_{SERS \text{ substrate}}}{I_{Silver \text{ on glass}}} \sim 4,400 \text{ (using Raman band @ } 1510 \text{ cm}^{-1}\text{)}$$

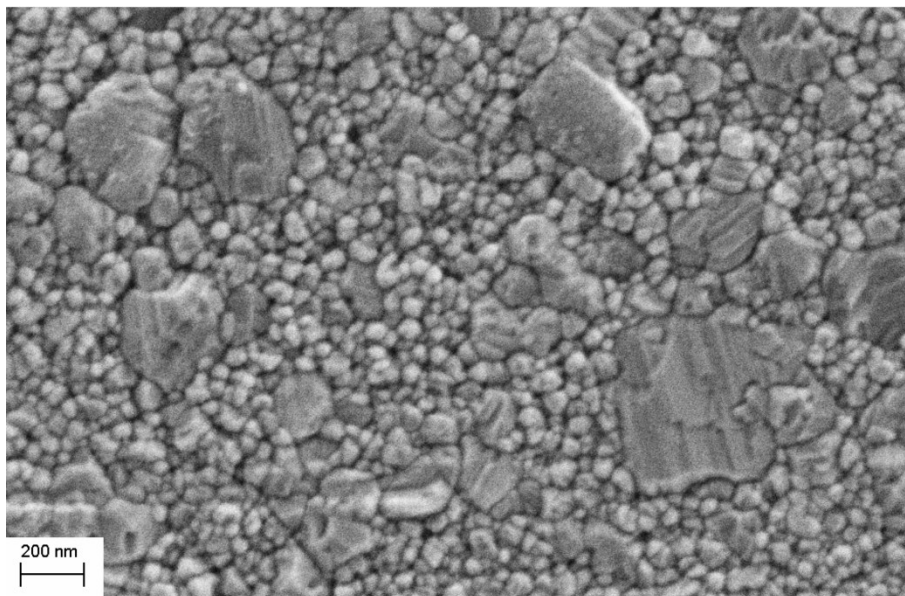


Figure S5g. Representative FESEM image of sputter coated silver film on glass slide. The scale bar represents 200 nm.

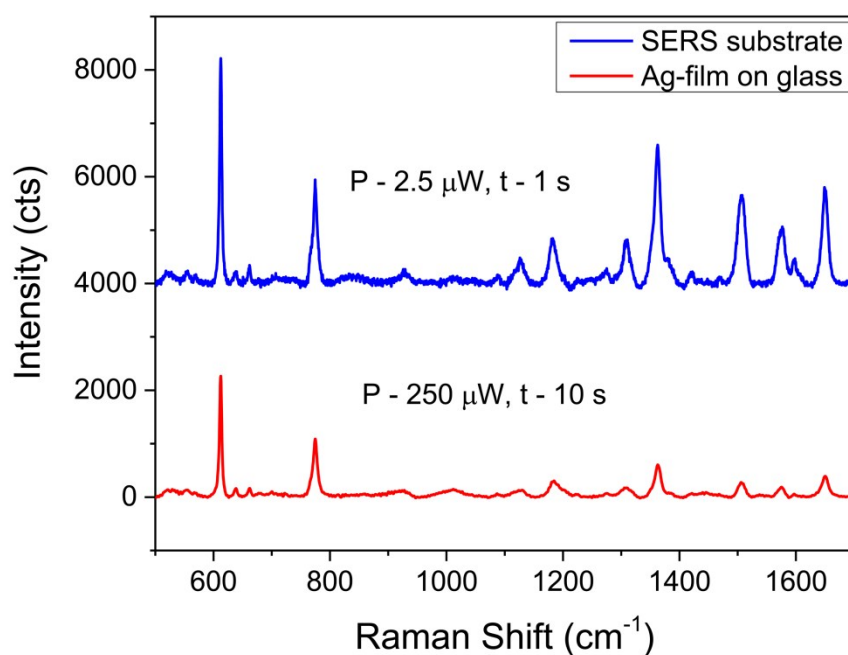


Figure S5h. Comparison of Raman signal from SERS substrate and sputter coated silver film on glass when dipped in 1mM R6G solution for 12 hours.

References:

1. Numerical Tool - COBRA <http://www.victoria.ac.nz/raman/publis/codes/cobra.aspx> (accessed Sep 1, 2015).
2. P. Hildebrandt and M. Stockburger, *J. Phys. Chem.*, 1984, **88**, 5935–5944.
3. E. C. Le Ru, E. Blackie, M. Meyer, P. G. Etchegoin, and E. C. Le Ru, *J. Phys. Chem. C*, 2007, **111**, 13794–13803.
4. K. Uetsuki, P. Verma, T. Yano, Y. Saito, T. Ichimura, and S. Kawata, *J. Phys. Chem. C*, 2010, **114**, 7515–7520.
5. L. Polavarapu, A. La Porta, S. M. Novikov, M. Coronado-Puchau, and L. M. Liz-Marzán, *Small*, 2014, **10**, 3065–71.
6. R. Sasai, T. Fujita, N. Iyi, H. Itoh, and K. Takagi, *Langmuir*, 2002, **18**, 6578–6583.
7. S. K. Sivaraman and V. Santhanam, *Nanotechnology*, 2012, **23**, 255603.
8. S. L. Kleinman, R. R. Frontiera, A.-I. Henry, J. A. Dieringer, and R. P. Van Duyne, *Phys. Chem. Chem. Phys.*, 2013, **15**, 21–36.